Fermi-LAT observations of the Crab nebula and pulsar

Marie-Hélène Grondin*† on behalf of the *Fermi*–LAT collaboration and the Pulsar Timing Consortium

*CNRS/IN2P3, Centre d'Études Nucléaires de Bordeaux Gradignan, UMR 5797, Gradignan, 33175, France,
†Université de Bordeaux, Centre d'Études Nucléaires de Bordeaux Gradignan, UMR 5797, Gradignan, 33175, France

***Abstract*. The Crab pulsar and nebula are the remnants of the supernova SN 1054. Previously detected by EGRET, both sources have been extensively studied in the gamma-ray energy band with the Large Area Telescope (LAT) aboard *Fermi*. LAT data were used to determine the Crab pulsar light curve and spectrum. The measurement of the cut-off energy at E_c = $(8.8 \pm 1.1\ ^{+2.9}_{-1.1})$ GeV, which could not be determined accurately in the EGRET era, allows better constraints of emission models, favouring a photon emission at high altitudes. A complete spectral analysis of the unpulsed gamma-ray emission in the 200 MeV – 300 GeV energy range is also performed. The spectrum of the nebula is well described by a power-law of spectral index $\Gamma = (1.89 \pm 0.04 \pm 0.10)$, that nicely connects with the observations from ground-based telescopes at about 100 GeV, thus providing constraints on physical parameters such as the magnetic field strength.**

***Keywords*: Crab, *Fermi*, gamma-rays, pulsar wind nebula, pulsar**

I. Introduction

The Crab nebula, the standard candle of astronomy, is the remnant of the supernova reported by the Chinese astronomers in 1054 A.D.. It is well studied all acrosss the electromagnetic spectrum. While synchrotron radiation is responsible for the observed emission below 200 MeV, inverse Compton scattering of the electrons off the synchrotron photons, far infra-red and CMB produces the high energy to very high energy gamma-rays.
Embedded in this nebula, PSR B0531+21, aka the Crab pulsar, is one of the most energetic pulsars, with a spin-down power of $\dot{E}$ = 4.6 $\times$ 10^{38} erg s^{-1}. Located at a distance of (2.0 $\pm$0.2) kpc, its period is $P = 33$ ms. Its characteristic age τ = P/2$\dot{P}$ = 1240 years, is close to the observationnal value.
Both the nebula and the pulsar have been extensively studied, in particular at high energy, with the Energetic Gamma-Ray Experiment Telescope (EGRET) [1], [2], [3], [4], in the 70 MeV –30 GeV energy band.
The Large Area Telescope (LAT), aboard the *Fermi* Gamma-ray Space Telescope, was successfully launched on June 11, 2008. With performance superior to EGRET's, it offers the opportunity to study the Crab high energy emission in more detail in the 20 MeV – 300 GeV energy range [5] and to better constrain emission models of the Crab pulsar and nebula. The results of 8 months of observations (August 3, 2008 to April 7, 2009) of the Crab region are reported here.

II. Radio timing

The Crab pulsar is young and noisy. An accurate timing solution is thus needed to know the rotational phase of the neutron star at each time, to derive precise gamma-ray phase histograms.
The timing solution of the Crab pulsar was obtained with the collaboration of the Nançay (France) ([6]) and Jodrell Bank (England) ([7]) radio telescopes, in the framework of the LAT pulsar timing campaign [8]. A total of 698 radio observations were performed between August 2008 and April 2009. No glitch was observed. Using the TEMPO2 pulsar timing package [9] and combining observations at 1.4 GHz and 600 MHz, residuals of 21 μs are obtained. A phase value is then assigned to each high energy photon.

III. Study of the gamma-ray light curves

Fermi-LAT data from August 3, 2008 to April 7, 2009 are considered here. Events from the "Diffuse" class are selected, i.e. the highest quality photon data, having the most stringent background rejection.
The pulsar is close to the Galactic plane. To maximize the signal (pulsed gamma-rays) to noise (background and nebular emission) ratio, photons in an energy-dependent region of interest are selected :

$$\theta < \mathrm{Max}(6.68 - 1.76\mathrm{Log}_{10}(\mathrm{E}_{\mathrm{MeV}}), 1.3)^{\circ} \qquad (1)$$

where θ is the angle between the photon direction and the pulsar radio position.
The temporal analysis is then performed on photons above 100 MeV. The resulting phase histogram is presented in Figure 1. Two distinct peaks, P1 and P2, can be clearly identified, at phases $\phi_1 \sim 0.988$ and $\phi_2 \sim 0.390$ respectively, both leading the radio peaks by $\delta\phi \sim 0.012$ in phase. In Figure 2, the data sample was divided in 5 different energy bands, showing the stability of the peak positions with the energy, while the P1/P2 ratio and the peak widths decrease with increasing energy.
From Figure 1, one defines the off-pulse window in the (0.52 – 0.87) pulse phase interval. This interval is then used in the study of the Crab nebula emission, due to the pulsar brightness in the rest of the phase interval.

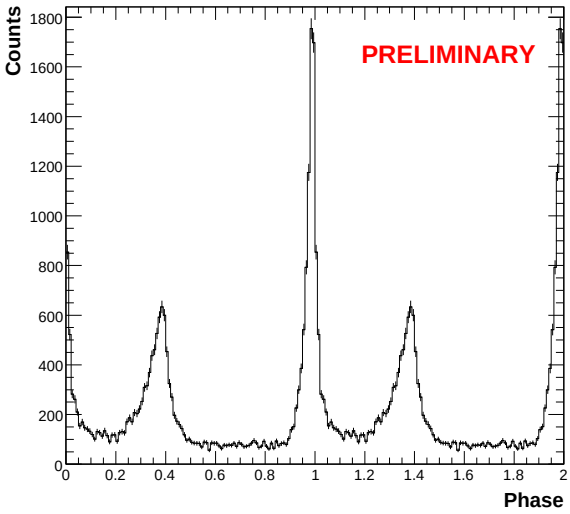

Fig. 1. Phase histogram of the Crab pulsar in an energy-dependent region and above 100 MeV. The main radio pulse is at phase 0. The light curve profile is binned to 0.01 of pulsar phase. Two cycles are shown. [10]

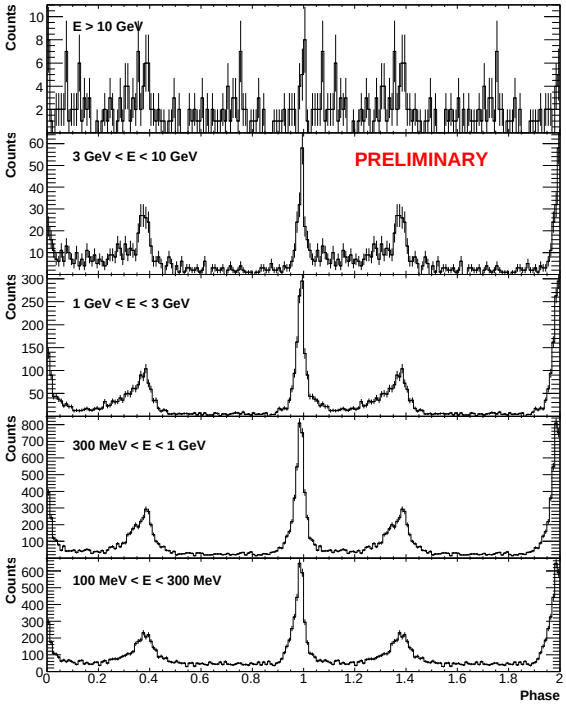

Fig. 2. Phase histograms in 5 different energy bands. Photons in an energy-dependent region and above 100 MeV are considered. The main radio pulse is at phase 0. The light curve profile is binned to 0.01 of pulsar phase. Two cycles are shown. [10]

IV. Spectral analysis

To accomodate uncertainties in the instrument response at low energy, still under investigation, only events above 200 MeV are selected for the spectral analysis of the Crab pulsar and nebula. A region of radius R = 20° around the pulsar radio position is considered, allowing a good estimation of the contributions of both the galactic and isotropic (extragalactic and instrumental) backgrounds.

A. The Crab nebula

Photons from the (0.52 – 0.87) off-pulse phase interval and above 200 MeV are considered here. Taking into account the brightest sources in the 20° region, a spectral study is performed, using the maximum-likelihood method [11]. The best fit is obtained with a power-law :

$$\frac{dN}{dE} = N_o(\frac{E}{10^3\mathrm{MeV}})^{-\Gamma}\,\mathrm{cm}^{-2}\,\mathrm{s}^{-1}\mathrm{MeV}^{-1} \qquad (2)$$

where N_o = (2.88 ± 0.14 ± 0.20) × 10^{-11} cm^{-2} s^{-1} MeV^{-1} is the prefactor determined on 35% of the total phase and Γ = (1.89 ± 0.04 ± 0.10) the spectral index. The corresponding flux above 200 MeV renormalized to the total phase is (1.35 ± 0.09 ± 0.20) × 10^{-7} cm^{-2} s^{-1}. The first error is statistical, whereas the second is due to systematic effects from the uncertainties in the effective area. No significant high-energy cut-off can be estimated with 8 months of data.

The *Fermi*-LAT spectral points, presented in Figure 3, provide a model-independent maximum likelihood spectrum, and agree well with the above fit (black line) and with EGRET results for the Crab nebula (green stars) [4]. Results of the Crab nebula spectrum obtained with Cherenkov telescopes (MAGIC : [12]; HESS : [13]; CANGAROO : [14]; VERITAS : [15]) are also overlaid. From this figure, the off-pulse source in the Crab region can be clearly identified as being the Crab nebula, since the *Fermi*/EGRET and Cherenkov spectral points link up naturally.

B. The Crab pulsar

The spectral study of the Crab pulsar uses the total phase interval, taking into account the nebular emission as a background component. Similarly to the case of the nebula, a maximum-likelihood method is applied on the photons above 200 MeV in a 20° region. The best fit of the pulsar energy distribution is obtained with an exponential cut-off power-law shape :

$$\frac{dN}{dE} = N_o(\frac{E}{10^3\mathrm{MeV}})^{-\Gamma} e^{-E/E_c}\,\mathrm{cm}^{-2}\,\mathrm{s}^{-1}\mathrm{MeV}^{-1}$$

where N_o = (2.13 ± 0.05 ± 0.08) × 10^{-10} cm^{-2} s^{-1} MeV^{-1} is the prefactor, Γ = (2.08 ± 0.02 ± 0.05) the spectral index and E_c = (8.8 ± 1.1 $^{+2.9}_{-1.1}$) GeV the cut-off energy of the distribution. The integral flux above 200 MeV is equal to (9.7 ± 0.1 $^{+1.1}_{-0.1}$) × 10^{-7} cm^{-2} s^{-1}.

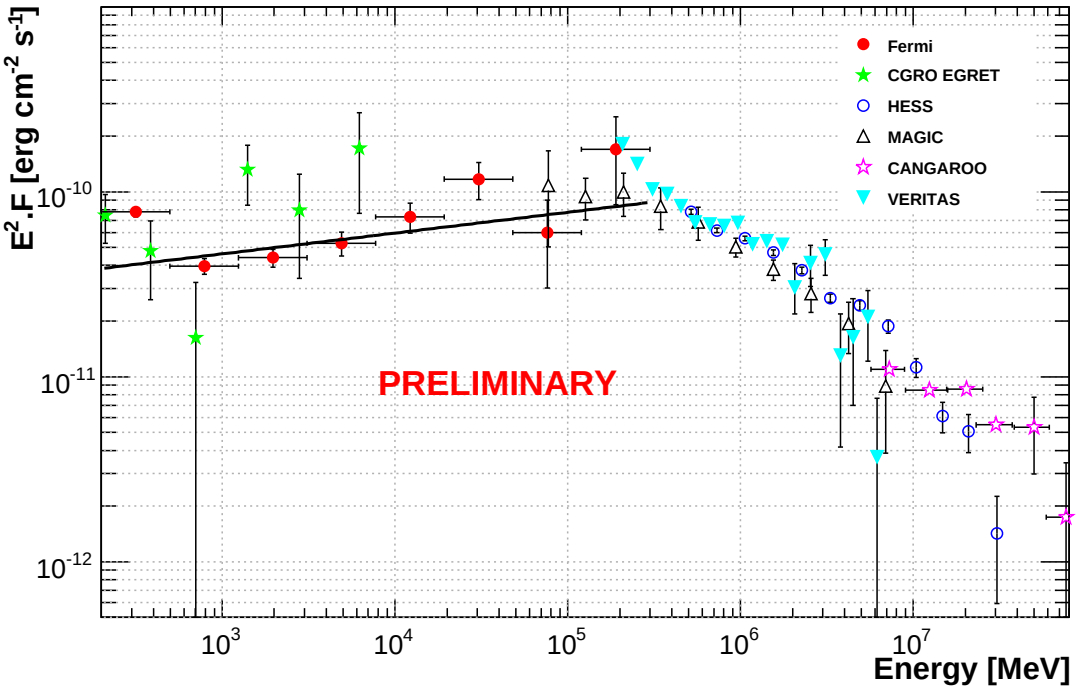

Fig. 3. Spectral energy distribution of the Crab nebula above 200 MeV. The fit on the total energy range (black line) and the *Fermi*-LAT spectral points (red points) are superimposed. Only statistical errors are shown. The horizontal error bars delimit the energy intervals. EGRET and Cherenkov results for the Crab nebula are also represented. References : CGRO EGRET : [4]; MAGIC : [12]; HESS : [13]; CANGAROO : [14]; VERITAS : [15]

The *Fermi*-LAT spectral points (red points) and the fit on the total energy range (black line) are presented in Figure 4 and agree well with EGRET (green stars) [4]. 95% upper limits were computed when the statistical significance of the energy interval was lower than 3 σ. We compute the probability of incorrect rejection of other spectral shapes using the likelihood ratio test. For instance, if only statistical errors are included, the power-law and hyper-exponential cut-off power-law[1] shapes are rejected at 10.7σ and 4.9σ, respectively.

The *Fermi*-LAT improved performance and the larger energy range compared to EGRET allow measurement of the cut-off energy of the pulsed spectral energy distribution, which was not possible with EGRET.

V. Discussion and conclusions

A. The Crab nebula

From Figure 3, the Crab nebula is firmly identified in the off-pulse window of the Crab pulsar. In a 200 MeV – 300 GeV energy range, it is well described by a power-law of spectral index $\Gamma = (1.89 \pm 0.04 \pm 0.10)$. No significant cut-off can be seen using 8 months of data.

[1]The power-law with an hyper-exponential cut-off is defined by the following function :

$$\frac{dN}{dE} = N_o(\frac{E}{10^3\mathrm{MeV}})^{-\Gamma} e^{(-(E/E_c)^b)}\,\mathrm{cm}^{-2}\,\mathrm{s}^{-1}\mathrm{MeV}^{-1}$$

where the exponent b is assumed to be equal to 2.

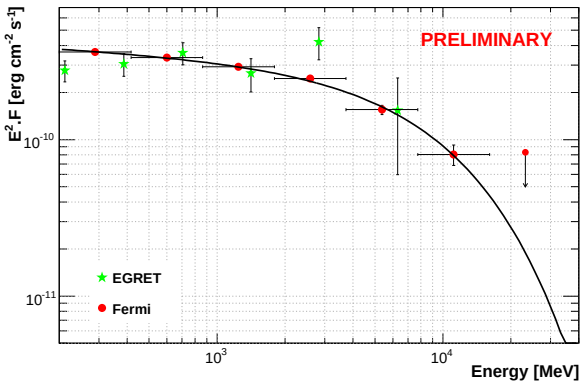

Fig. 4. Spectral energy distribution of the Crab pulsar above 200 MeV. The fit on the total energy range (black line) and the *Fermi*-LAT spectral points (red points) are superimposed. Only statistical errors are shown. The horizontal error bars delimit the energy intervals. EGRET results (green stars) are also represented.

The *Fermi*-LAT and Cherenkov experiments cover the energy range in which the self-synchrotron Compton scattering dominates. Therefore, studies in collaboration between *Fermi* and ground-based telescopes should allow us to better constrain the cut-off or break energy of the inverse Compton component, visible in Figure 3 around 100 GeV.

As presented in [16], the Crab nebula is one of the best candidates to perform a cross-calibration between *Fermi* and ground-based experiments, allowing these latter to

reduce their systematic uncertainties. This study could be performed with more data, within a few months.

B. The Crab pulsar

The high energy study of the Crab is an opportunity to better constrain the theoretical models decribing the emission coming from pulsars. They can be sorted in two classes. On one hand, the Polar Cap model (PC) describes an emission at low altitude and close to the neutron star surface, and should be characterized by an hyper-exponential cut-off power-law shape in the *Fermi*-LAT energy range. On the other hand, the Outer Gap model (OG) consists of high energy photon emission between the null charge surface and the light cylinder. A third scenario, the Two Pole Caustic model (TPC) predicts emission in slot gaps located between the neutron star surface and the light cylinder along the last open field line.

The light curves of the Crab pulsar show two distinct peaks, P1 and P2 at phases $\phi_1 \sim 0.988$ and $\phi_2 \sim 0.390$ respectively, whose positions are stable with energy and separated by $\Delta\phi \sim 0.402$, and leading the radio main pulses by $\delta\phi \sim 0.012$ in phase. The P1/P2 ratio and the widths of the peaks decrease with increasing energy.

The precise measurement of the shape of the pulsed emission spectrum and its cut-off energy in the *Fermi* range is possible thanks to the instrument sensitivity and the large covered energy range. The best fit is a simple exponential cut-off power-law, and cannot be explained by a polar cap scenario. The obtained value of the cut-off : E_c = $(8.8 \pm 1.1\ ^{+2.9}_{-1.1})$ GeV can be compared to the result recently published by the MAGIC collaboration [17] : E_c = $(17.7 \pm 2.8 \pm 5.0)$ GeV, based on the EGRET spectrum. They are marginally consistent, taking into account the systematic errors.

Following [18], the maximum energy of pulsed photons can constrain the lower bound of altitude emission. We can use the observed cut-off energy to estimate a minimum emission height as $r \geq (\epsilon_{max} B_{12}/1.76\,\mathrm{GeV})^{2/7} P^{-1/7} R_*$, where ϵ_{max} is the unabsorbed photon energy, P is the spin period and the surface magnetic field is $10^{12} B_{12}$ G. For the Crab pulsar, one obtains $r \geq 4.7 R_*$, which excludes any emission close to the neutron star surface.

The gamma-ray efficiency η =$L_\gamma/\dot{E}$ is the part of the spin-down power $\dot{E}$ which is converted to gamma-ray luminosity L_γ. This latter is defined by : $L_\gamma = 4\pi f_\Omega F_{obs} D^2$, where F_{obs} is the observed phase-averaged energy flux over 200 MeV, D = 2 kpc is the distance to the pulsar and f_Ω is a correction factor that takes into account the beaming geometry, depending on the magnetic inclination angle α and the Earth viewing angle ζ. For the Crab, we assume $f_\Omega \sim 1$. The LAT results yield an efficiency of the order of $\eta \sim 0.1\%$ above 200 MeV, which is consistent with the heuristic luminosity law mentioned in [19], [8], [20], according to which $\eta \propto \dot{E}^{-1/2}$ and verified by several gamma-ray pulsars.

ACKNOWLEDGMENTS

The *Fermi* LAT Collaboration acknowledges generous ongoing support from a number of agencies and institutes that have supported both the development and the operation of the LAT as well as scientific data analysis. These include the National Aeronautics and Space Administration and the Department of Energy in the United States, the Commissariat à l'Energie Atomique and the Centre National de la Recherche Scientifique / Institut National de Physique Nucléaire et de Physique des Particules in France, the Agenzia Spaziale Italiana and the Istituto Nazionale di Fisica Nucleare in Italy, the Ministry of Education, Culture, Sports, Science and Technology (MEXT), High Energy Accelerator Research Organization (KEK) and Japan Aerospace Exploration Agency (JAXA) in Japan, and the K. A. Wallenberg Foundation, the Swedish Research Council and the Swedish National Space Board in Sweden.

Additional support for science analysis during the operations phase from the following agencies is also gratefully acknowledged: the Istituto Nazionale di Astrofisica in Italy and the K. A. Wallenberg Foundation in Sweden for providing a grant in support of a Royal Swedish Academy of Sciences Research fellowship for JC.

The Nançay Radio Observatory is operated by the Paris Observatory, associated with the French Centre National de la Recherche Scientifique (CNRS). The Lovell Telescope is owned and operated by the University of Manchester as part of the Jodrell Bank Centre for Astrophysics with support from the Science and Technology Facilities Council of the United Kingdom.

REFERENCES

[1] Nolan, P.L. et al., 1993, ApJ, 409, 697
[2] de Jager, 0.C.. et al., 1996, ApJ, 457, 253
[3] Fierro, J.M. et al., 1998, ApJ, 494, 734
[4] Kuiper, L. et al., 2001, A&A, 378, 918
[5] Atwood, W.B. et al., 2009, ApJ, 697, 1071
[6] Theureau, G. et al., 2005, A&A, 430, 373
[7] Hobbs, G.B. et al., 2004, MNRAS, 353,1311
[8] Smith, D.A., et al., 2008, A&A, 492, 923
[9] Hobbs, G.B. et al., 2006, MNRAS, 369,655
[10] Abdo, A.A. et al., 2009, *in preparation*
[11] Mattox, J.R. et al., 1996, ApJ, 461, 396
[12] Albert, J. et al., 2008, ApJ, 674, 1037
[13] Aharonian, F.A. et al., 2006, A&A, 457, 899
[14] Tanimori, T. et al., 1997, arXiv/9710272
[15] Celik, O., 2007, arXiv/0709.3868v1
[16] Bastieri, D. et al., 2005, APh, 23, 572
[17] Aliu, E. et al., 2008, arXiv/0809.2998
[18] Baring, M.G. 2004, Adv. Sp. Res., 33, 552
[19] Arons, J., 1996, A&A Suppl. Ser., 120, 49
[20] Watters, K.P. et al., 2009, ApJ, *submitted* (arXiv/0812.3931)